

Electronic Supplementary Information

One-Pot Surface Engineering of Battery Electrode Materials with Metallic SWCNT-Enriched, Ivy- Like Conductive Nanonets

*JongTae Yoo,^{†a} Young-Wan Ju,^{†b} Ye-Ri Jang,^{†a} Ohhun Gwon,^a Sodam Park,^a Ju-Myung Kim,^a
Chang Kee Lee,^c Sun-Young Lee,^d Sun-Hwa Yeon,^{*e} Guntae Kim,^{*a} and Sang-Young Lee^{*a}*

^a Department of Energy Engineering, School of Energy and Chemical Engineering, Ulsan National Institute of Science and Technology (UNIST), Ulsan 44919, Korea

^b Department of Chemical Engineering, College of Engineering, Wonkwang University, Iksan 54538, Korea.

^c Korea Packaging Center, Korea Institute of Industrial Technology, Ojeong-gu, Bucheon 14449, Korea

^d Department of Forest Products, Korea Forest Research Institute, Seoul 02455, Korea

^e Energy Storage Laboratory, Korea Institute of Energy Research (KIER), Daejeon 34129, Korea

[†]These authors contributed equally.

Correspondence and requests for materials should be addressed to S. -H. Yeon^e (email: ys93@kier.re.kr), G. Kim^a (email: gtkim@unist.ac.kr) and S. -Y. Lee^a (email: syleek@unist.ac.kr)

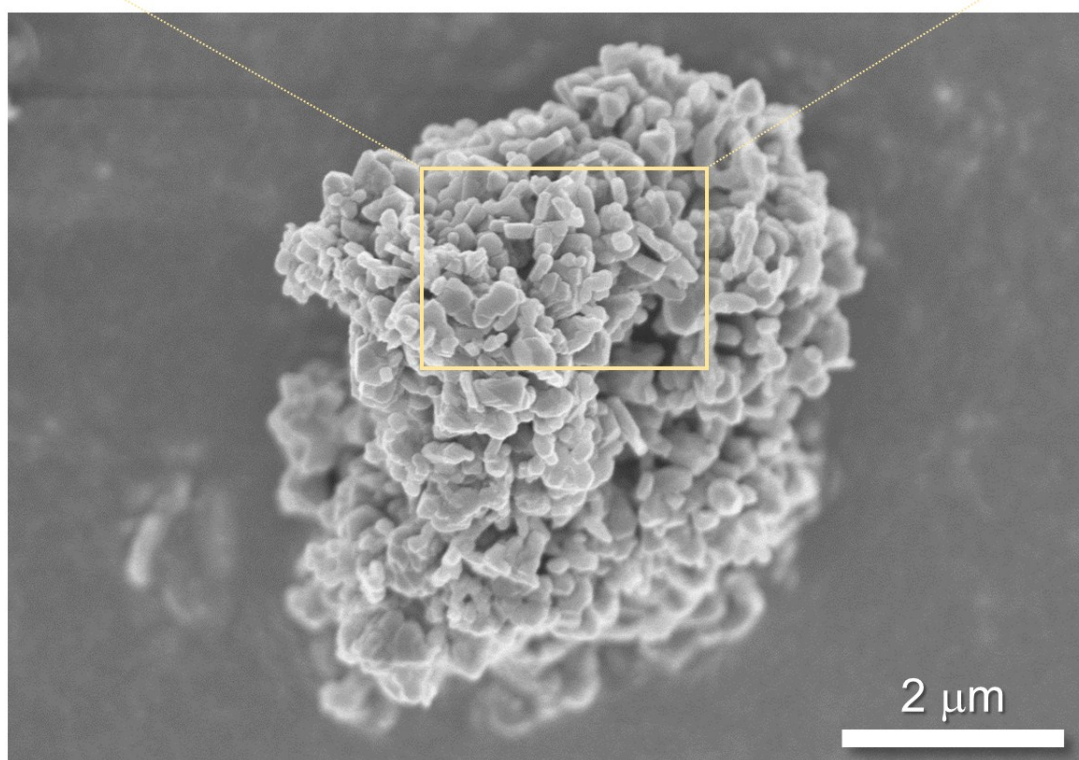
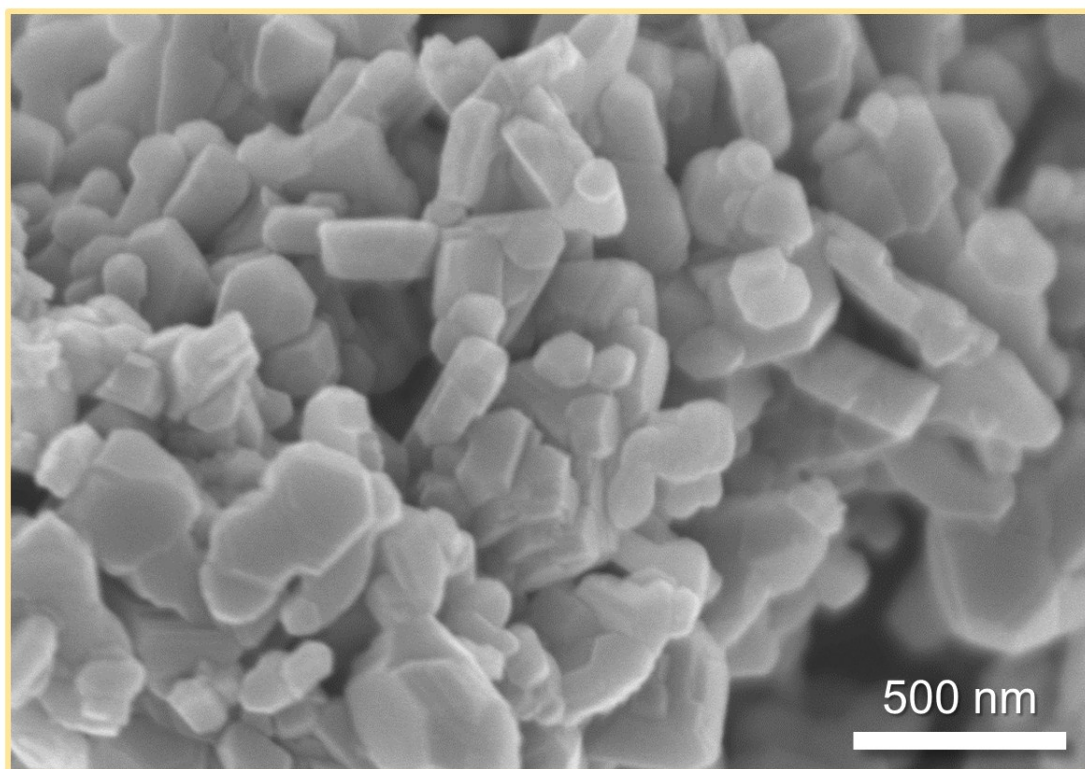


Figure S1. SEM images of the pristine OLO.

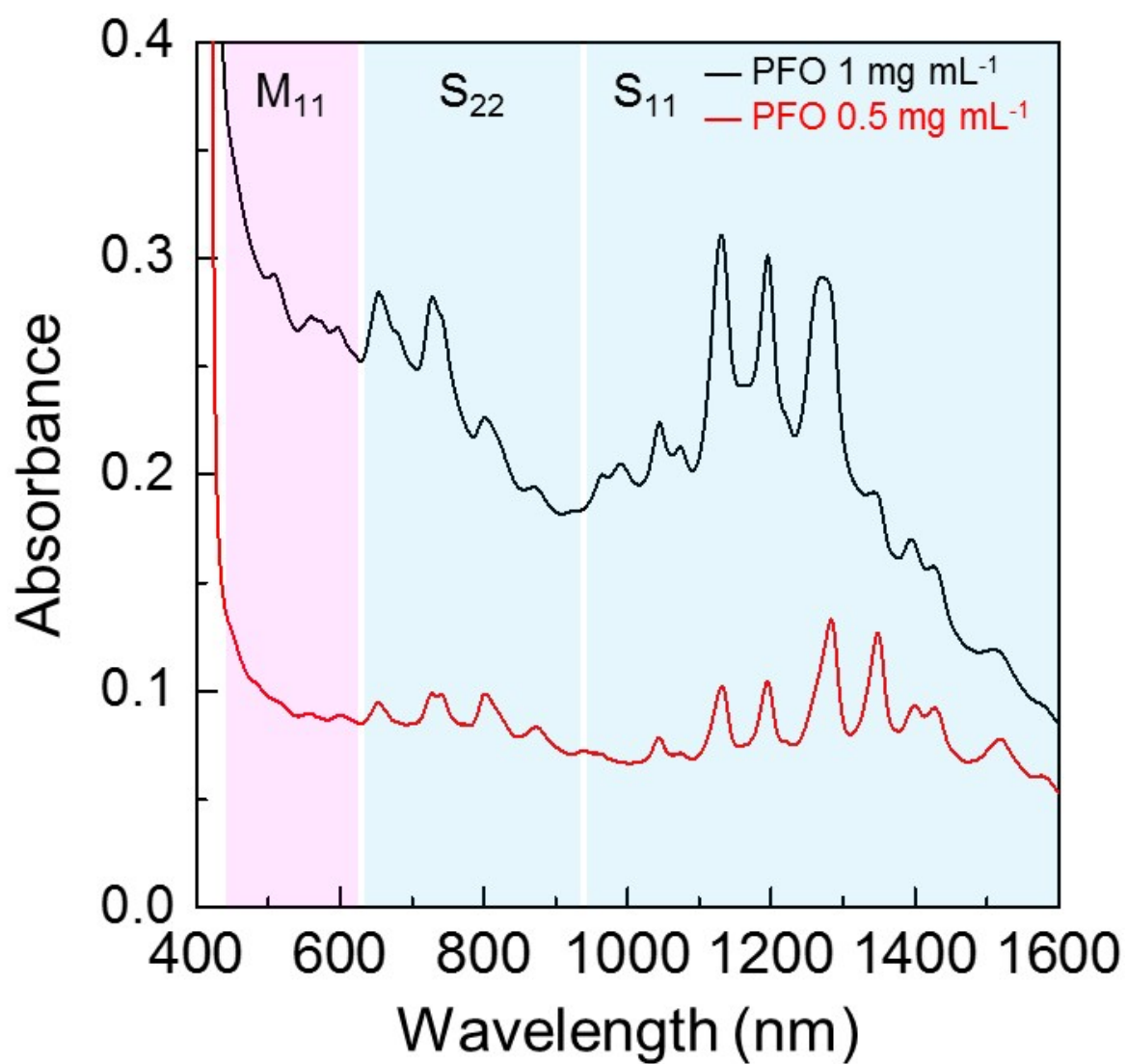


Figure S2. UV-vis-NIR spectra of the supernatants of PFO-dissolved SWCNT/OLO suspensions as a function of the initial PFO concentration.

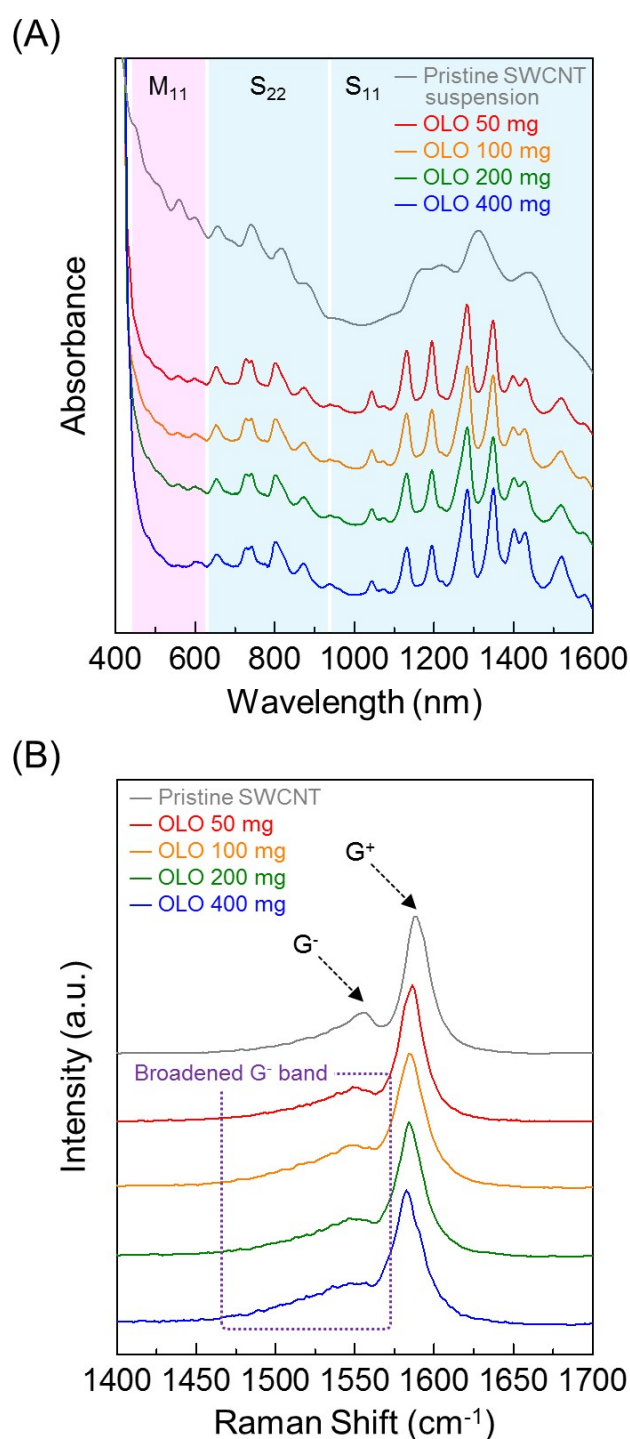


Figure S3. (A) UV-vis-NIR spectra of the supernatants of the SWCNT/OLO suspensions with PFO as a function of the initial OLO content in the PFO (0.5 mg mL^{-1})-dissolved SWCNT (1 mg)/OLO suspension. The pristine SWCNT suspension (dispersed without PFO in NMP) was examined as a control sample. (B) Raman spectra showing the G-band peaks of the OLO@mSC as a function of the initial OLO content in the PFO (0.5 mg mL^{-1})-dissolved SWCNT (1 mg)/OLO suspension. Pristine SWCNTs were examined as the control sample.

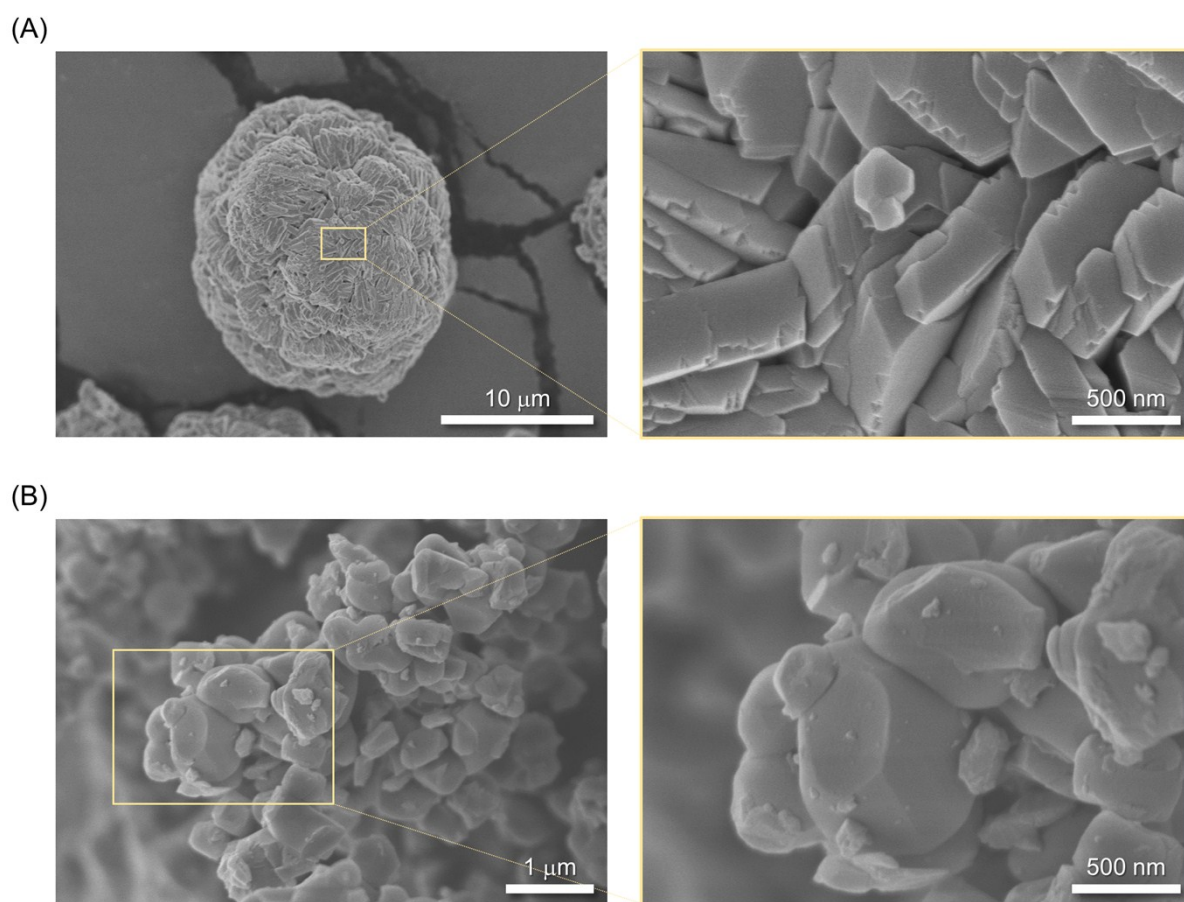


Figure S4. SEM images of the pristine (A) LNMO and (B) LTO.

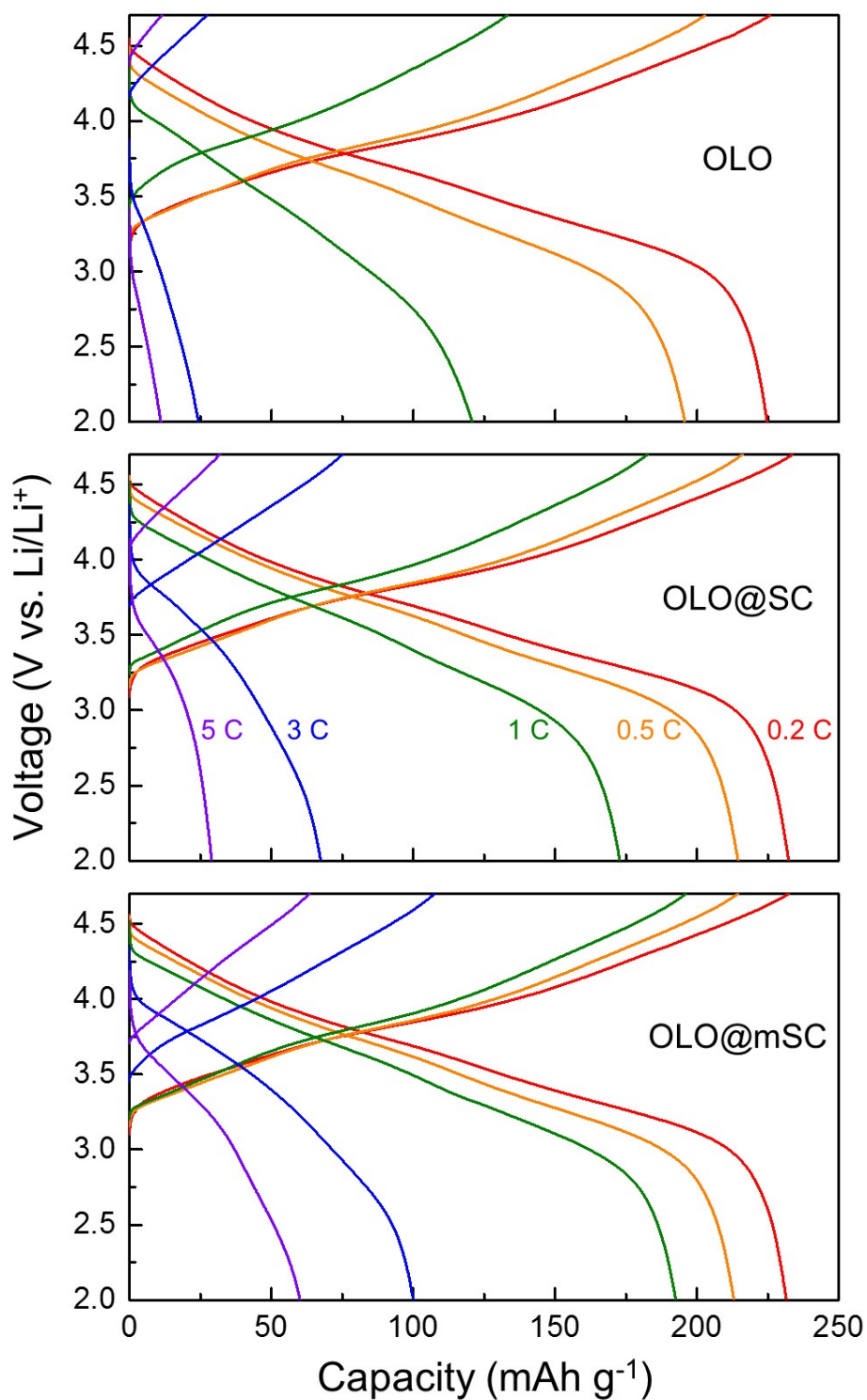


Figure S5. Charge/discharge profiles of the pristine OLO (top), OLO@SC (middle), and OLO@mSC (bottom) cathodes, wherein the cells were charged at a constant current density of 0.2 C (= 0.34 mA cm⁻²) and discharged at various current densities ranging from 0.2 to 3.0 C.

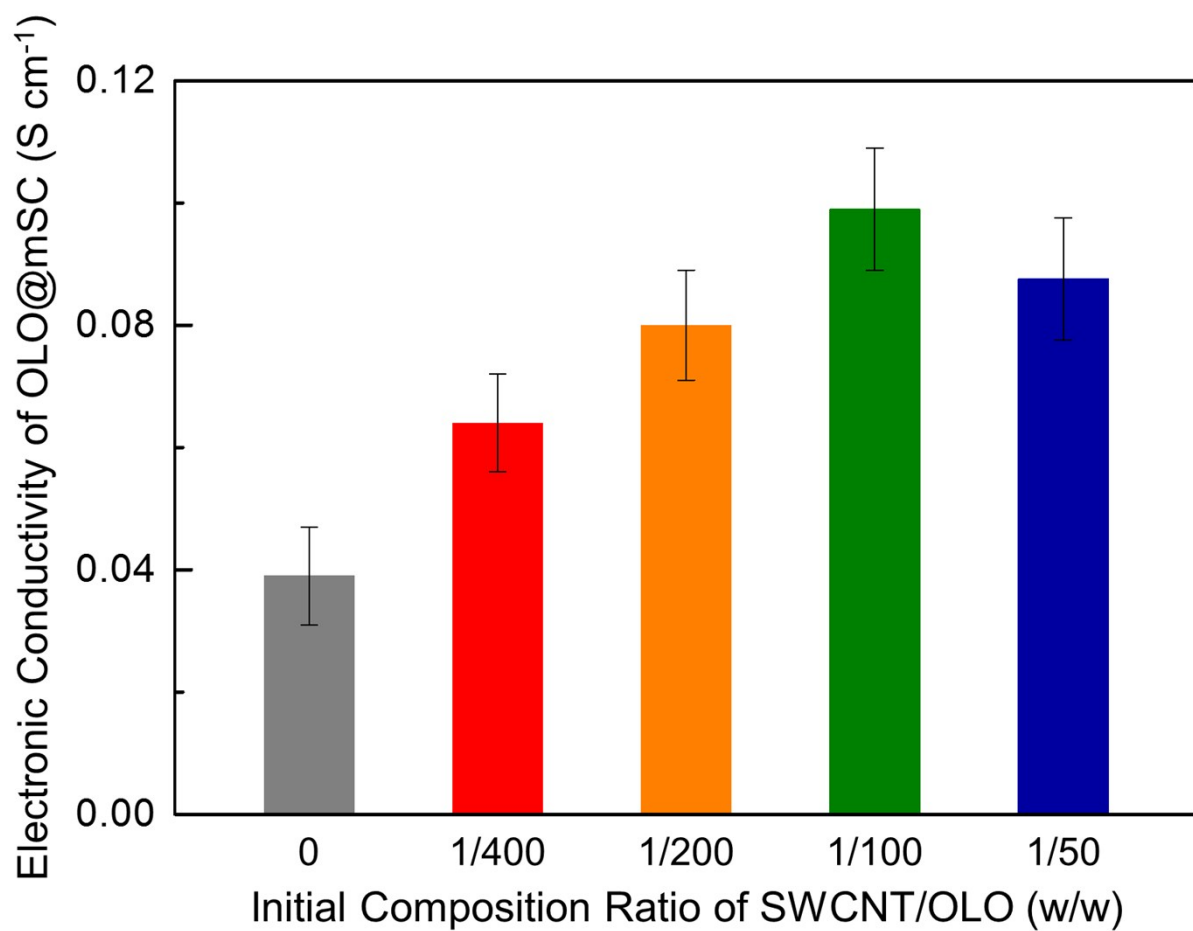


Figure S6. Comparison of the electronic conductivity of the OLO@mSC cathodes as a function of the initial composition ratio of SWCNT/OLO in the suspensions.

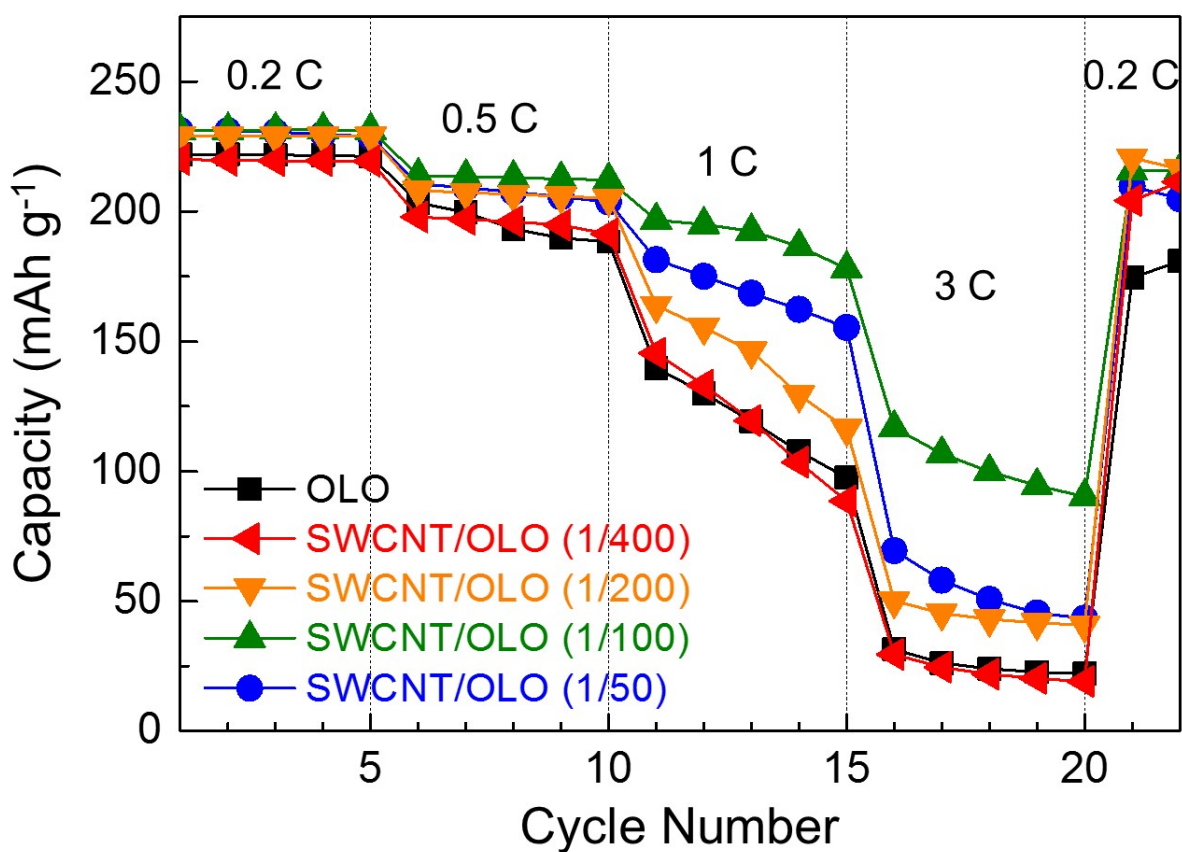


Figure S7. Discharge rate performance of the OLO@mSC cathodes as a function of the initial composition ratio of SWCNT/OLO in the suspension, wherein the cells were charged at a constant current density of 0.2 C ($= 0.34 \text{ mA cm}^{-2}$) and discharged at various current densities ranging from 0.2 to 5.0 C.

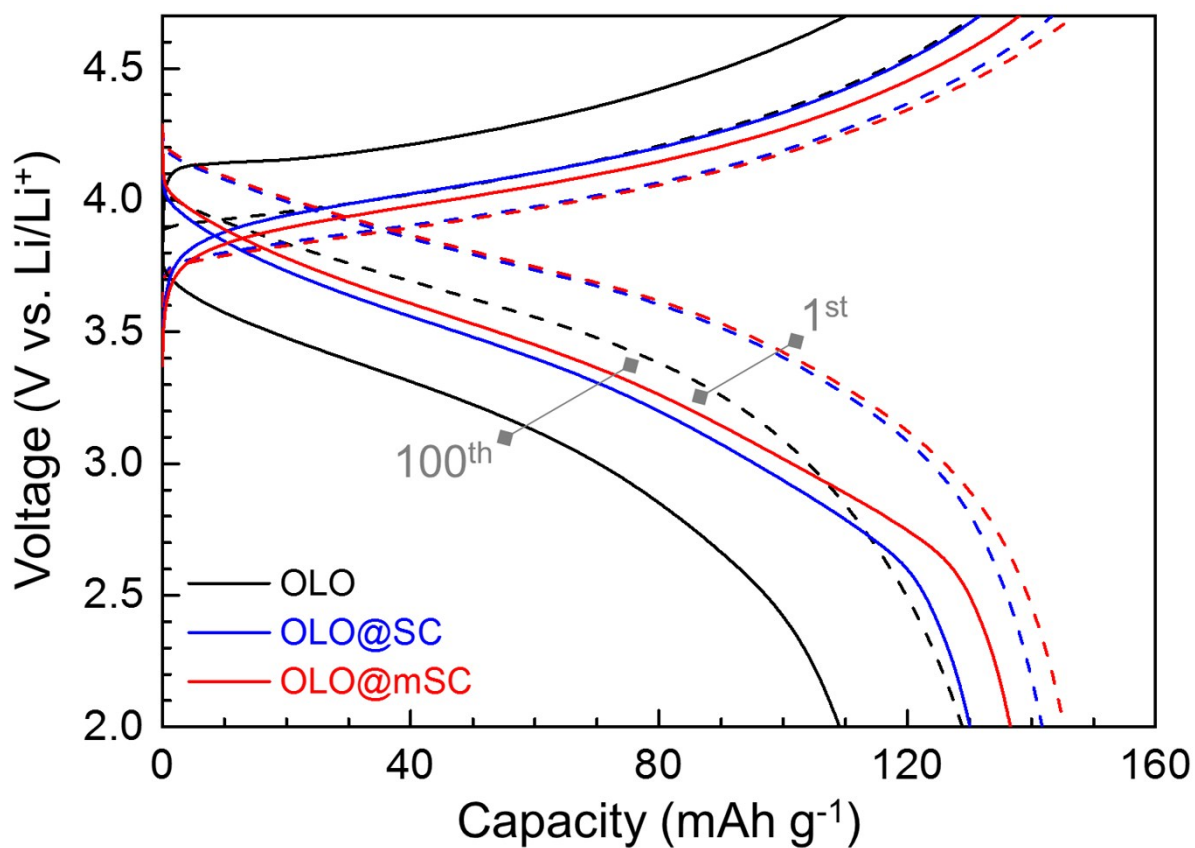


Figure S8. Charge/discharge profiles (for the 1st and 100th cycles) of the pristine OLO, OLO@SC, and OLO@mSC cathodes, wherein the cells were cycled at a charge/discharge current density of 5.0 C/5.0 C under voltage range of 2.0 – 4.7 V.

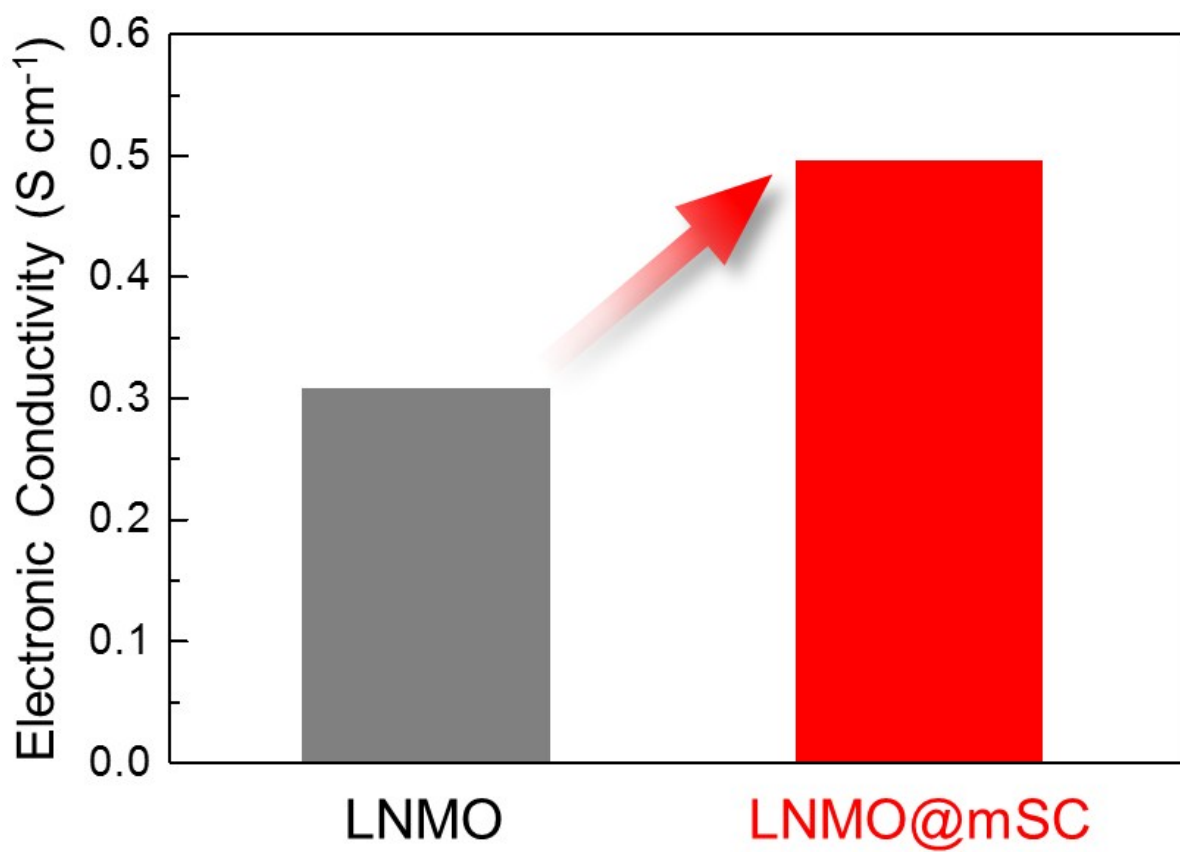


Figure S9. Comparison of the electronic conductivity between the pristine LNMO and LNMO@mSC.

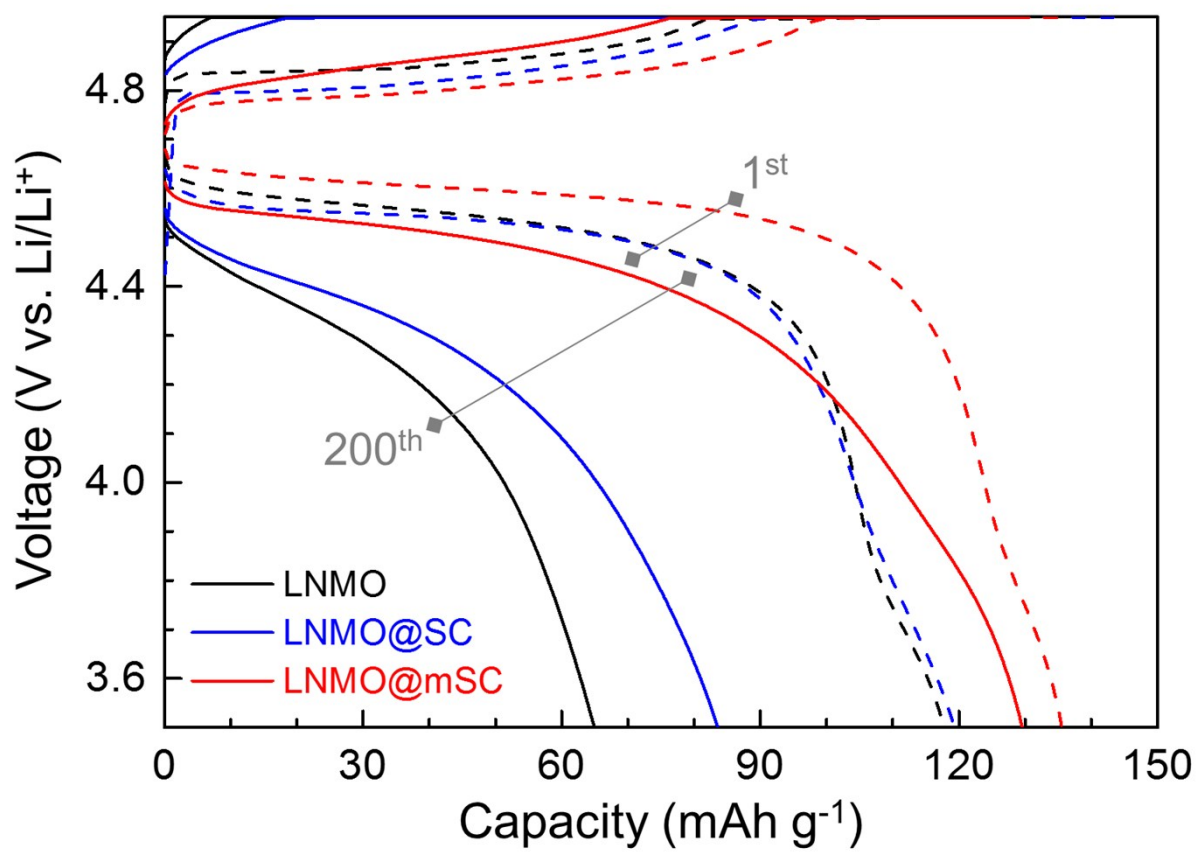


Figure S10. Charge/discharge profiles (for the 1st and 200th cycles) of the pristine LNMO, LNMO@SC, and LNMO@mSC cathodes, wherein the cells were cycled at a charge/discharge current density of 5.0 C/5.0 C under voltage range of 3.5 – 4.95 V.

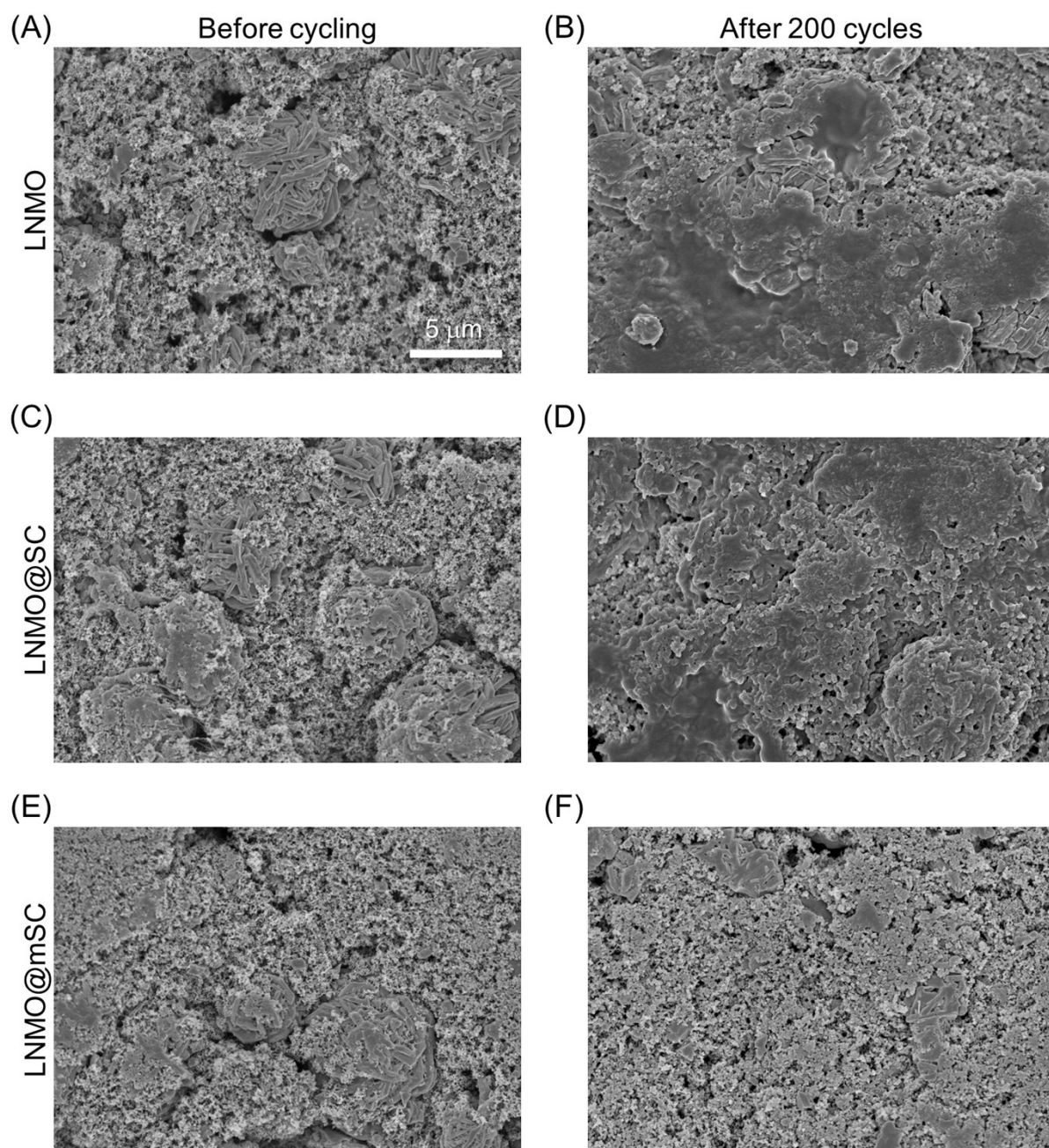


Figure S11. SEM images of the (A,B) pristine LNMO, (C,D) LNMO@SC, and (E,F) LNMO@mSC cathodes (A,C,E) before and (B,D,F) after the 200th cycle, wherein the cells were cycled at a charge/discharge current density of 5.0 C/5.0 C under voltage range of 3.5 – 4.95 V.

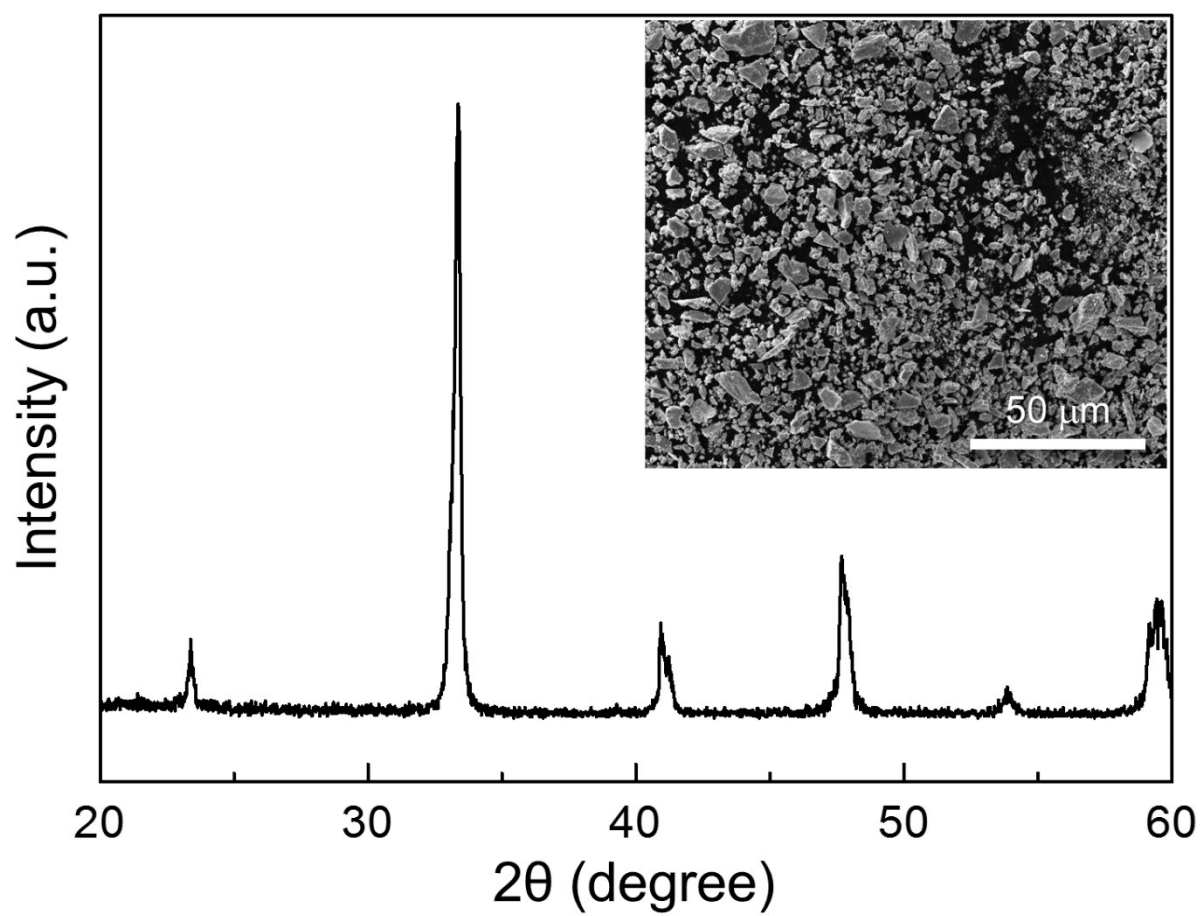


Figure S12. XRD pattern and SEM image (inset) of the as-synthesized NSC powders.

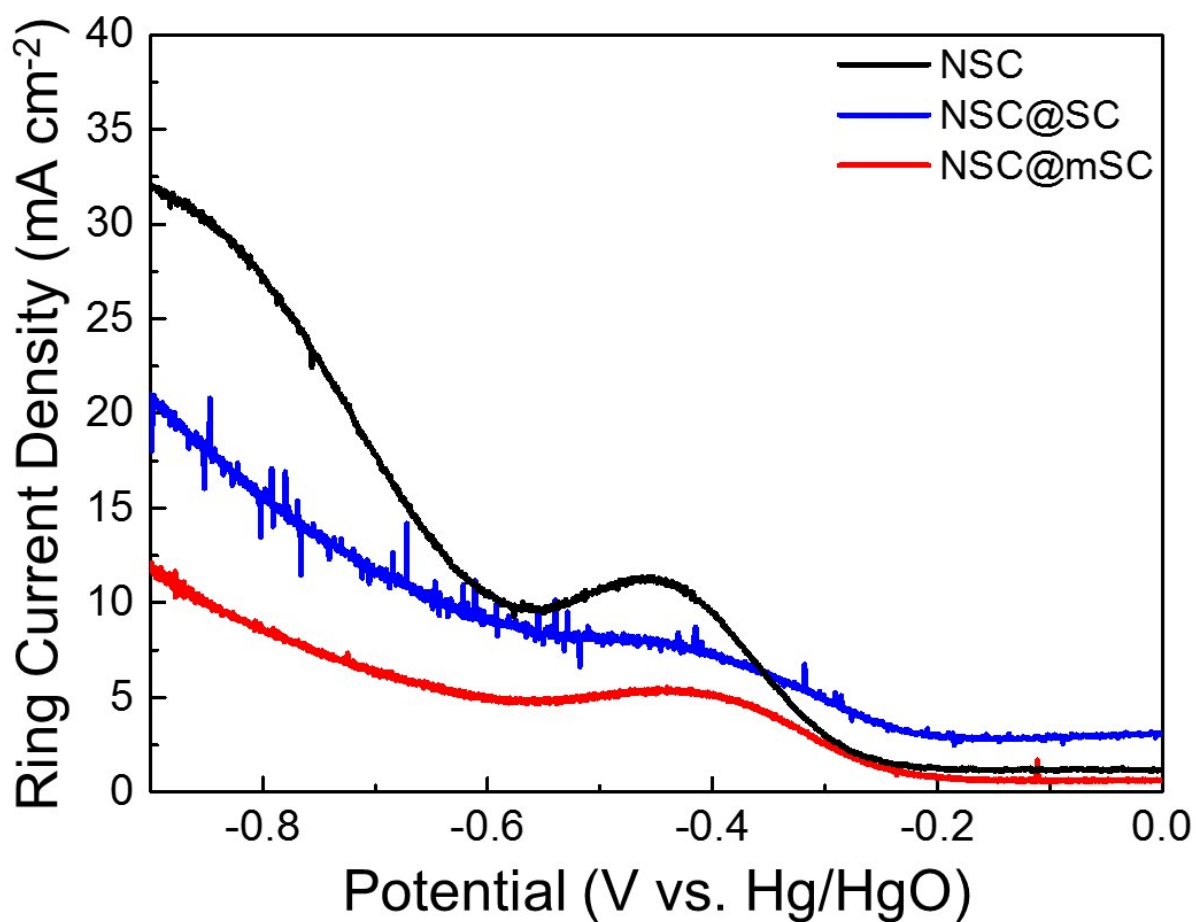


Figure S13. Ring current density profiles of NSC, NSC@SC, and NSC@mSC, which were investigated using RRDE measurements in an oxygen-saturated 0.1 M KOH aqueous solution (catalyst loading = 1.0 g cm⁻², scan rate = 10 mV s⁻¹, rotating rate = 1600 rpm).

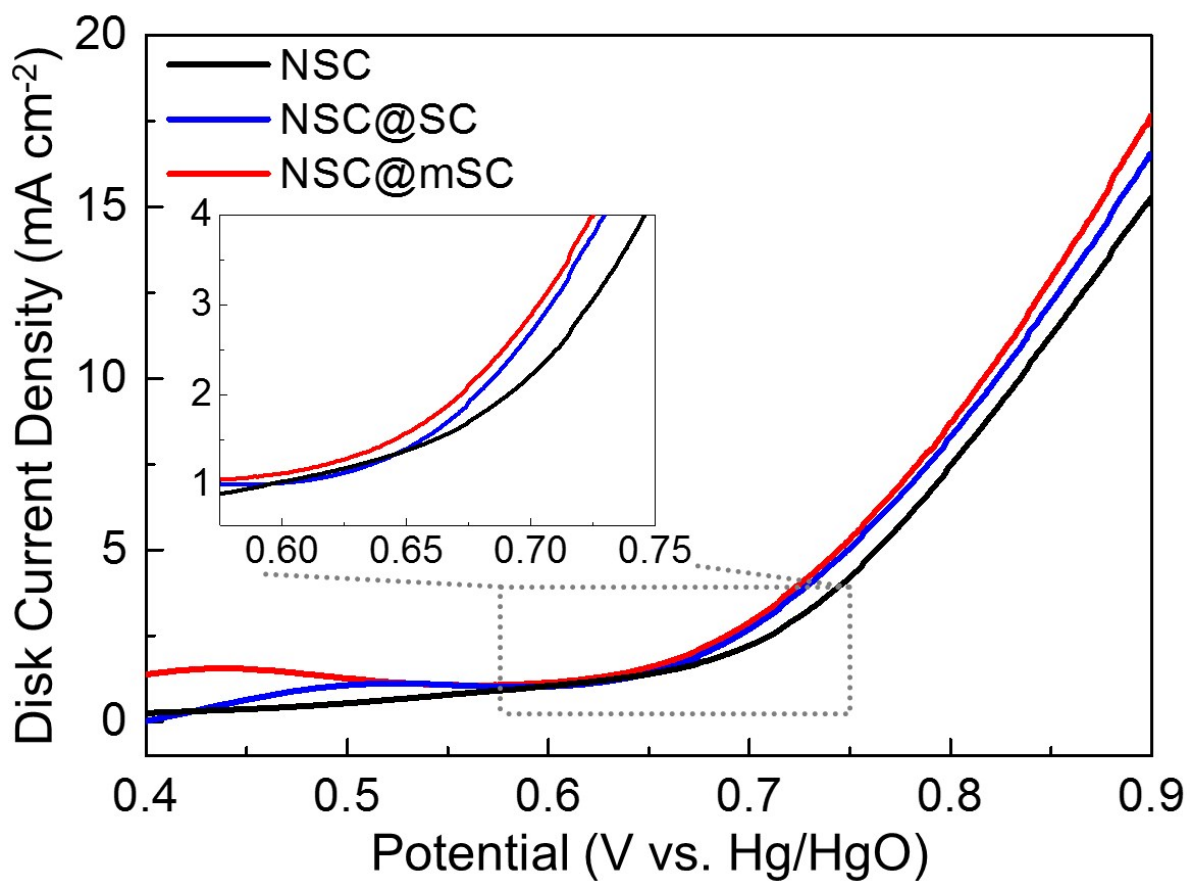


Figure S14. OER polarization curves of NSC, NSC@SC, and NSC@mSC, which were investigated using the RRDE measurements in an oxygen-saturated 0.1 M KOH aqueous solution (catalyst loading = 1.0 g cm⁻², scan rate = 10 mV s⁻¹, rotating rate = 1600 rpm).

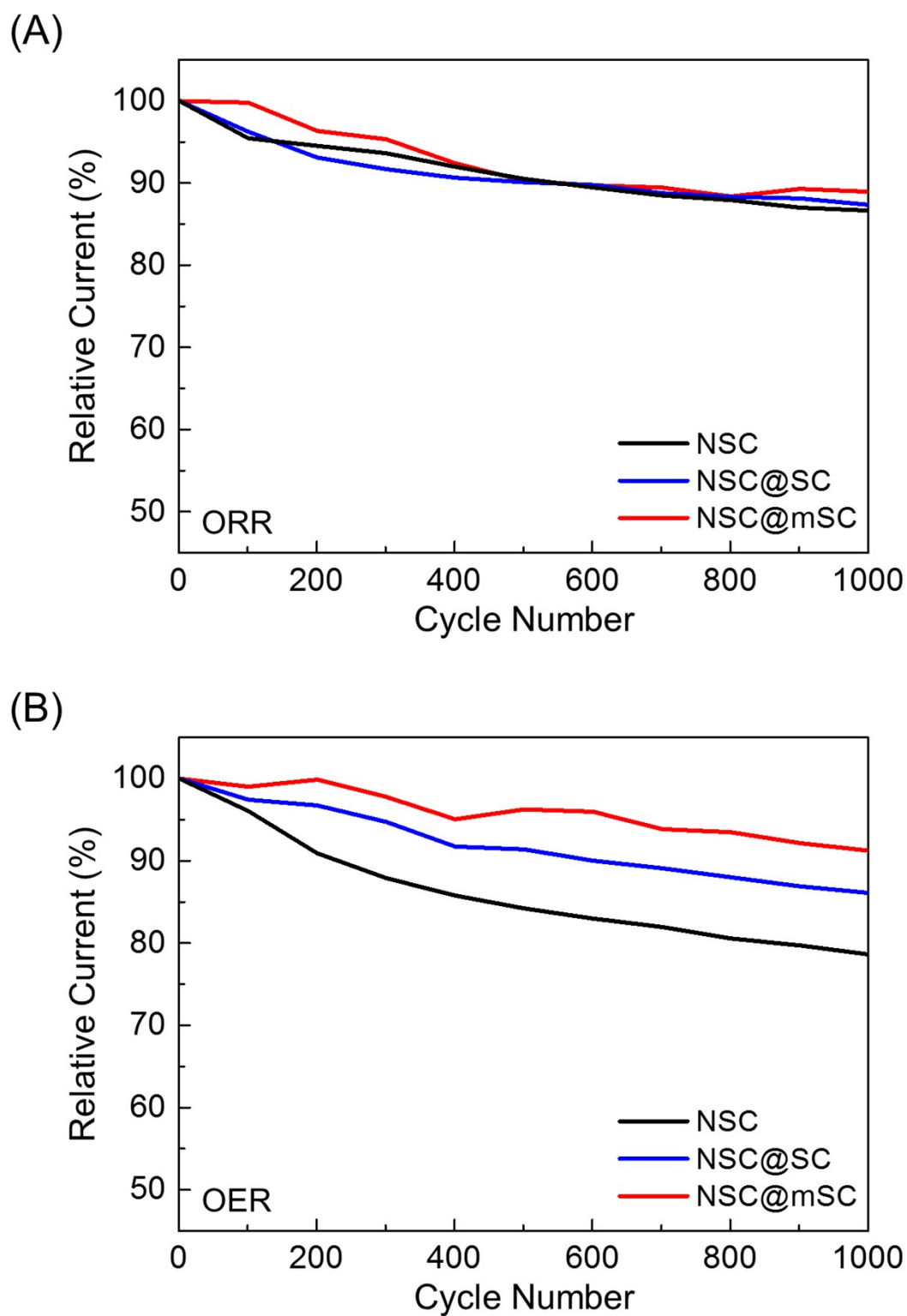


Figure S15. (A) ORR and (B) OER relative current of NSC, NSC@SC, and NSC@mSC respectively collected at -0.9 and 0.9 V for 1000 cycles, which were investigated using the RRDE measurements in an oxygen-saturated 0.1 M KOH aqueous solution (scan rate = 100 mV s^{-1} , rotating rate = 1600 rpm).

Table S1. Comparison of composite ratio, areal mass loading, areal capacities, and capacity retention for OLO cathodes (This work vs. Previous studies).

Publication <u>/Engineering method</u>	Composite ratio (%)			Mass loading (mg cm ⁻²)	Capacity (mAh g _{cathode} ⁻¹)	Areal capacity (mAh cm ⁻²)	Capacity retention (%) at RT
	Active material	Conductive agent	Binder				
This work <u>/metallic SWCNT-enriched coating</u>	92	4	4	7	213 (at 0.2C)	1.62	94.0 (100th) (at 5C/5C)
<i>J. Power Sources</i> , 2016, 327 , 273. <u>/Boron doping</u>	80	10	10	3.7	220 (at 0.1C)	1.02	89.9 (50 th) (at 0.2C/0.2C)
<i>Adv. Sci.</i> , 2016, 3 , 1600184. <u>/AlF₃-coated heterostructure</u>	80	10	10	4.5	170 (at ~0.3C)	0.96	98.0 (100 th) (at ~0.3C/0.3C)
<i>Adv. Energy Mater.</i> , 2015, 5 , 1500274. <u>/Inorganic surface coating</u>	80	10	10	4.5	204 (at 0.1C)	1.15	84.3 (110 th) (at 1C/1C)
<i>J. Mater. Chem. A</i> , 2015, 3 , 17113. <u>/F_{0.3}-SnO₂ (FTO) coating</u>	80	10	10	2	237 (at 0.1C)	0.59	83.0 (300 th) (at ~0.3C/0.3C)
<i>J. Mater. Chem. A</i> , 2015, 3 , 13933. <u>/Mesoporous Al₂O₃-polyacene coating</u>	85	10	5	3	251 (at 0.1C)	0.89	95.0 (100 th) (at 1C/1C)
<i>ACS Appl. Mater. Interfaces</i> , 2014, 6 , 21711. <u>/AlF₃ coating</u>	80	10	10	3	200 (at 0.1C)	0.75	87.9 (50 th) (at 0.1C/0.1C)
<i>Adv. Energy Mater.</i> , 2013, 3 , 1299. <u>/Atomic layer deposition (TiO₂)</u>	80	10	10	2.9	230 (at 0.1C)	0.83	78.0 (50 th) (at ~0.3C/0.3C)

Table S2. Comparison of composite ratio, areal mass loading, areal capacities, and capacity retention for LNMO cathodes (This work vs. Previous studies).

Publication <u>/Engineering method</u>	Composite ratio (%)			Mass loading (mg cm ⁻²)	Capacity (mAh g _{cathode} ⁻¹)	Areal capacity (mAh cm ⁻²)	Capacity retention (%)
	Active material	Conductive agent	Binder				
This work <u>/metallic SWCNT-enriched coating</u>	85	7.5	7.5	7	116 (at 0.2C)	0.95	97.3 (200th) (at 5C/5C)
<i>Adv. Funct. Mater.</i> , 2017, 27 , 1602873. <u>/Al₂O₃ coating</u>	80	10	10	3.5	115 (at 0.2C)	0.50	-
<i>J. Mater. Chem. A</i> , 2017, 5 , 145. <u>/Incorporation of Li₇La₃Zr₂O₁₂ (LLZO)</u>	80	10	10	2.1	102 (at 0.1C)	0.27	95.9 (300 th) (at 0.5C/1C)
<i>ACS Appl. Mater. Interfaces</i> , 2016, 8 , 9116. <u>/Cr and Nb doping</u>	82	10	8	3.1	107 (at 0.2C)	0.40	94.1 (500 th) (at 1C/1C)
<i>J. Mater. Chem. A</i> , 2015, 3 , 15457. <u>/RuO₂ coating</u>	80	10	10	2.3	96	0.28	14.4* (1000 th) (at 1C/1C)
<i>J. Power Sources</i> , 2015, 274 , 1254. <u>/Atomic layer deposition (Al₂O₃)</u>	90	5	5	5.5	113 (at 0.1C)	0.69	98.0 % (150 th) (at 0.5C/0.5C)
<i>ACS Appl. Mater. Interfaces</i> , 2015, 7 , 16231. <u>/TiO₂ and Al₂O₃ coating</u>	100	0	0	0.81	106 (at ~0.1C)	0.09	-

* = Approximately calculated values

Table S3. Comparison of catalytic activities for ORR/OER bifunctional catalysts (This work vs. Previous studies).

Publication	Electrocatalyst	Electron transfer number for ORR (n)	Peroxide yield for ORR (%)	OER relative current (%)
This work	Perovskite (Nd_{0.5}Sr_{0.5}CoO_{3-δ}) modified by metallic-enriched SWCNTs	3.83 – 3.91	< 9	91 after 1,000 cycles (at 100 mV s⁻¹)
<i>Nano Energy</i> , 2017, 31 , 541.	NiCo ₂ S ₄ nanocrystal anchored on N-doped CNTs	~3.80	< ~10	-
<i>J. Mater. Chem. A</i> , 2016, 4 , 2122.	Perovskite (Nd _{0.5} Sr _{0.5} CoO _{3-δ}) coated by I-doped graphenes	3.68* – 3.80	< 10	~95* after 10 cycles (at 10 mV s ⁻¹)
<i>J. Mater. Chem. A</i> , 2016, 4 , 4516.	Pt/C-LiCoO ₂ composites	~3.92	< 4	86 after 50 cycles (at 10 mV s ⁻¹)
<i>Danton Trans.</i> , 2016, 45 , 18494.	Cubic α-Mn ₂ O ₃ prisms	3.55* – 3.71*	< ~20*	~50* after 300 cycles (at 10 mV s ⁻¹)
<i>Adv. Energy Mater.</i> , 2015, 5 , 1501560.	Perovskite (Ba _{0.5} Sr _{0.5} Co _x Fe _{1-x} O _{3-δ}) with amorphous thin layers	3.59 – 3.71	< ~23*	-
<i>Angew. Chem. Int. Ed.</i> , 2014, 53 , 4582.	Perovskite (La _{0.3} (Ba _{0.5} Sr _{0.5}) _{0.7} Co _{0.8} Fe _{0.2} O _{3-δ})	~3.72	< 20	-

* = Approximately calculated values